Molecular Dynamics Simulation of Monoalkyl Glycoside Micelles in Aqueous Solution: Influence of Carbohydrate Headgroup Stereochemistry

Teoh T. Chong,[†] Rauzah Hashim,[†] and Richard A. Bryce*[,‡]

Department of Chemistry, University of Malaya, 50603 Kuala Lumpur, Malaysia, and School of Pharmacy and Pharmaceutical Sciences, University of Manchester, Manchester M13 9PL, U.K.

Received: November 25, 2005; In Final Form: January 19, 2006

Comparative molecular dynamics simulations of *n*-octyl-β-D-galactopyranoside (β-C_8Gal) and *n*-octyl-β-D-glucopyranoside (β-C_8Glc) micelles in aqueous solution have been performed to explore the influence of carbohydrate stereochemistry on glycolipid properties at the atomic level. In particular, we explore the hypothesis that differences in T_m and T_c for β-C_8Gal and β-C_8Glc in lyotropic systems arise from a more extensive hydrogen bonding network between β-C_8Gal headgroups relative to β-C_8Glc, due to the axial 4-OH group in β-C_8Gal. Good agreement of the 13 ns micelle−water simulations with available experimental information is found. The micelles exhibit a similar shape, size, and degree of exposed alkyl chain surface area. We find net inter- and intra-headgroup hydrogen bonding is also similar for β-C_8Gal and β-C_8Glc, although *n*-octyl-β-D-galactopyranoside micelles do exhibit a slightly greater degree of inter- and intra-headgroup hydrogen bonding. However, the main distinction in the calculated microscopic behavior of β-C_8Glc and β-C_8Gal micelles lies in solvent interactions, where β-D-glucosyl headgroups are considerably more solvated (mainly at the equatorial O4 oxygen). These results agree with preceding theoretical and experimental studies of monosaccharides in aqueous solution. A number of long water residence times are found for solvent surrounding both micelle types, the largest of which are associated with surface protrusions involving headgroup clusters. Our simulations, therefore, predict differences in hydrogen bonding for the two headgroup stereochemistries, including a small difference in inter-headgroup interactions, which may contribute to the higher T_m and T_c values of β-C_8Gal surfactants relative to β-C_8Glc in lyotropic systems.

1. Introduction

Glycolipids possess a polar carbohydrate headgroup linked to a hydrophobic alkyl tail. As amphiphilic molecules, glycolipids are capable of demonstrating liquid crystalline phase behavior. In a biological context, glycolipids are found in a fluid lamellar L_α phase in cell membranes alongside phospholipids, forming inhomogeneous domains, asymmetric with respect to the inner and outer membrane leaves.[1] The carbohydrate moieties exhibit mechanical and recognition functions. Specific carbohydrate residues are recognized in the adhesion of signaling molecules (e.g., integrins)[2] or pathogens (e.g., cholera toxin).[3] Glycolipids are distinct from phospholipids such as phosphatidylcholine in having a nonionic headgroup, which experiences shorter-range and less repulsive electrostatic interactions. As nonionic compounds, surfactants such as *n*-octyl-β-D-glucopyranoside have been utilized in the solubilization of membrane proteins without loss of function, for physical characterization.[4,5] With the implication in molecular recognition processes, glycolipid surfactants are also attractive as a vector for liposomal drug delivery.[6,7] An interesting recent use of *n*-octyl-β-D-glucopyranoside has been in providing a chiral template for the formation of helical polymers,[8] a process thought to be guided by specific hydrogen bonding interactions. Glycolipids exhibit good biodegradability[9] and can be obtained directly from natural sources such as sago and oil palm, although purity is an issue. They are however readily synthesizable from renewable resources such as fatty alcohols and oligosaccharides.[10]

It is therefore important to determine the factors controlling the structural and physical properties of glycolipids. However, due to the complexity of carbohydrate headgroups, the relationship between chemical structure and properties is not well understood.[10] Small variations in saccharide headgroup dictate phase behavior. An example is given by monoalkyl glycosides such as *n*-octyl-β-D-glucopyranoside (which we subsequently denote β-C_8Glc, using the notation of Sakya et al.[11]). β-C_8Glc exhibits thermotropic liquid crystal behavior, with a melting temperature, T_m, of 342 K and a clearing temperature, T_c, of 380 K for transition to the isotropic phase, L_1.[11−14] The surfactant *n*-octyl-β-D-galactopyranoside (β-C_8Gal) differs from β-C_8Glc solely in the stereochemistry at the C4 position on the monosaccharide headgroup (Figure 1). This epimer, however, exhibits significantly higher melting and clearing points, of 369 and 400 K, respectively.[11] A similar trend in relative T_m and T_c is observed for the phase behavior of the two mesomorphic glycolipids in lyotropic systems.[11] The molecular basis for this difference in physical properties is not known. Clearly, for these lipids, where the tail length is relatively short, the properties of the liquid crystalline phases depend strongly on the detailed interactions of the polar headgroups with neighboring headgroups and, in the case of lyotropic systems, with water molecules.

It has been proposed that the difference in T_m and T_c for β-C_8Gal and β-C_8Glc in thermotropic and lyotropic systems may be related to differences in hydrogen bond networks: specifi-

* Corresponding author. E-mail: R.A.Bryce@manchester.ac.uk. Fax: (0)161-275-2481. Phone: (0)161-275-8345.
[†] University of Malaya.
[‡] University of Manchester.

10.1021/jp056851g CCC: $33.50
Published on Web 02/15/2006

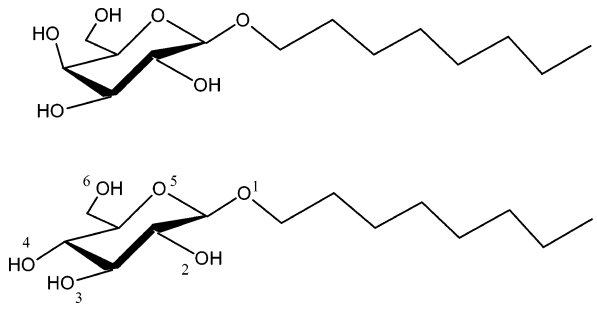

Figure 1. (top) *n*-Octyl-β-D-galactopyranoside (β-C_8Gal) and (below) *n*-octyl-β-D-glucopyranoside (β-C_8Glc) with atom labeling scheme.

cally, that there may be more extensive hydrogen bonding between β-C_8Gal headgroups relative to β-C_8Glc, due to a more-exposed 4-OH group in β-C_8Gal.[11] In the absence of crystal structures of anhydrous β-C_8Gal or β-C_8Glc or their hydrates, molecular dynamics (MD) simulations are well placed to provide detailed information on intermolecular interactions present in these glycolipid systems and give insight into the basis of their differing physical behavior. Indeed, MD simulations have proved a powerful tool in studies of the structural and dynamic characteristics of mono- and disaccharides in aqueous solution,[15−17] as well as glycolipid bilayers[18,19] and micelles.[18,20] For example, MD simulations were used to compare the microscopic behavior of *n*-decyl-α-D-glucopyranoside and *n*-decyl-β-D-glucopyranoside monolayers at the water−decane interface.[21] These calculations have suggested that increased tilt of the α-glucose headgroups leads to poorer packing of the decyl chains, providing a molecular basis for the propensity of *n*-decyl-α-D-glucopyranoside to form large, nonspherical assemblies in preference to the smaller, more typical micellar sizes exhibited by the β-anomer.[21,22]

In this work, we use atomistic MD simulations to computationally probe the inter-saccharide, intra-saccharide, and saccharide−solvent hydrogen bond networks of β-C_8Gal and β-C_8Glc micelles in a uniformly hydrated environment. Specifically, we explore the hypothesis of increased inter-headgroup interactions for the β-C_8Gal surfactant relative to its β-C_8Glc epimer. In addition, we study the effect of stereochemistry more generally on solvent and micelle shape, structure, and stability.

2. Methods

2.1. Model. The β-D-glucosyl and β-D-galactosyl headgroups were modeled using the all-atom GLYCAM_2000 force field.[23,24] After van Buuren et al.,[21] alkyl chains were described using a nonelectrostatic model, with all-atom parameters adopted from Cornell et al.[25] Water was modeled using the TIP3P potential.[26] In building a micelle−water system to simulate isobaric−isothermal conditions, a suitable number of lipids is required a priori. Aggregation numbers for β-C_8Glc range between 21 and 65 at 298 K.[4,27] For simulation using atomistic potentials, we constructed a 27-lipid micelle, an aggregation number corresponding to an experimental estimate.[28] This is in approximate agreement with a simple packing constraint calculation, using the expression $n = 2\pi r^2/A_{head}$.[29] For an all-trans chain length of 4 × 2.54 Å and an additional 2.54 Å for the headgroup, a radius, r, of 12.7 Å is obtained. Using an estimated[13] headgroup area, A_{head}, of 44 Å^2, an estimated aggregation number, n, of 23 is calculated. Thus, we note that an aggregate number of 27 may exist toward the upper limit for an ideal spherical micelle. Initial micelle models for β-C_8Gal and β-C_8Glc were constructed using rigid-body rotation of extended lipid conformations, to form an evenly spaced spherical micelle. The micelle was then immersed in an octahedron of pre-equilibrated solvent, with initial dimensions of $a = b = c = 54.5$ Å and $\alpha = \beta = \gamma = 109.5°$. Octahedral periodic boundary conditions give uniform and efficient solvation of globular systems such as micelles. After immersion, this system comprised 27 surfactants and 2190 water molecules. The formal micelle concentration was 0.6 M, or 83 wt % water, considerably above the critical micelle concentrations in water (∼29.5 mM for β-C_8Gal and ∼18−20 mM for β-C_8Glc).[30] As discussed by Bogusz et al.,[18] restrictions in inter-micelle interactions due to the imposed periodic boundary conditions obviate micelle aggregation at high concentrations. Thus, the effective concentration is considerably below the formal concentration and should have a minimal effect on calculated properties.

2.2. MD Simulations. MD simulations were performed using the AMBER 8.0 suite of programs.[31] Long-range electrostatics employed a particle-mesh Ewald method for octahedral periodic boundary conditions. Nonbonded interactions were truncated at 8 Å. Simulations were performed under conditions of constant temperature and pressure (we note that use of the isokinetic Berendsen thermostat entails approximating an isobaric−isothermal ensemble), using a value of 0.2 ps for both thermostat and barostat coupling constants.[32] A time step of 2 fs was used, in conjunction with the SHAKE algorithm,[33] to constrain the distances of covalent bonds involving hydrogen.

The micelles were subjected to rounds of heating and cooling using harmonic constraints on the terminal C atom of the chains (Figure 1). The micelles were then heated without constraints from 0 to 300 K over 100 ps and subsequently equilibrated at 300 K for 500 ps. Production MD simulations for β-C_8Gal or β-C_8Glc were performed for 13 ns at 300 K and 1 atm, with coordinates archived every 0.2 ps.

2.3. Analysis. Calculation of radii of gyration and hydrogen bond analysis was performed using the *carnal* and *ptraj* modules of AMBER, respectively. Hydrogen bond analysis used a O···O distance cutoff of 4 Å and an angle tolerance of 60° from linearity. Standard errors were estimated from block averaging. Under the assumption of an ellipsoidal micelle shape, the eccentricity, e, was computed from $(1 - c^2/a^2)^{1/2}$, where a and c are the ellipsoid dimensions along the longest and shortest semiaxes, respectively. Calculation of e employed in-house software, as did calculation of local density profiles and water residence times. Residence times were calculated using configuration step sizes of 0.2 and 2.0 ps, to reflect the fact that water molecules may at an instant librate beyond the 4 Å cutoff and yet remain proximal to the solute oxygen. Solvent-accessible surface areas of aggregates were obtained using the program NACCESS,[34] an implementation of the method of Lee and Richards,[35] with radii of 1.8, 0.0, and 1.4 Å for C, H, and O, respectively, and a probe radius of 1.4 Å.

3. Results

3.1. Stability of Micelle Structure. We first consider the stability of β-C_8Gal and β-C_8Glc micelles over the course of the 13 ns simulations. The micelles remained intact over the duration of the trajectories. The presence of expected[36] periodic near-escape events by surfactants was observed. The rough micelle surface, with protrusion of glycolipids, is apparent from inspection of MD configurations (Figure 2). Typically, prior to partial protrusion from the micelle, the lipid involved adopted a surface orientation where both tail and headgroup were largely solvent-exposed. Subsequent interactions with other lipids then drew the near-escaped surfactant back into a similar solvent-

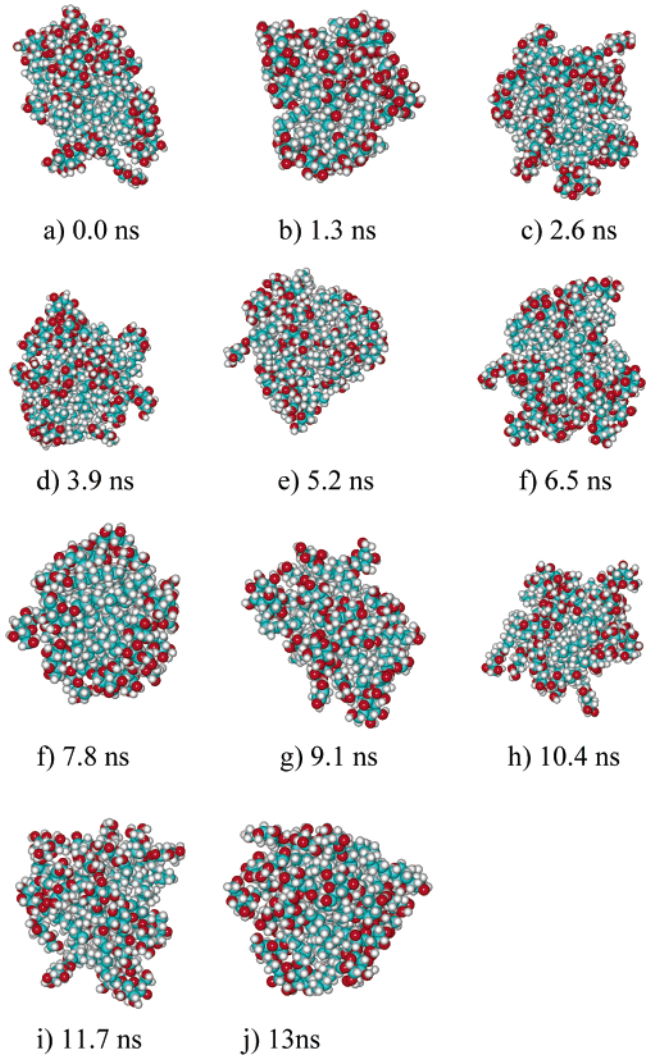

Figure 2. Time series of MD snapshots of β-C_8Glc micelles over a 13 ns simulation. Oxygen (red), carbon (cyan), and hydrogen (white) atoms are shown.

exposed pose or into a more buried-tail orientation. However, full escape events were not seen on the nanosecond time scale of the simulations (experimentally, lipid exchange occurs in the microsecond regime).[29]

Size. The radius of gyration, R_g, was calculated over 13 ns (Figure 3). For both surfactants, R_g displays a gradual downward drift until it stablizes after 5 ns. This compaction is particularly apparent for the (β-C_8Glc)$_{27}$ micelle, where the 2.5 ns block average R_g value decreases by 0.12 Å over the first 5 ns of the 13 ns trajectory; this decrease in block average is reduced to 0.02 Å for the final 5 ns, indicating stabilization of R_g. Averaging over this final 5 ns of production trajectory, a R_g value of 12.36 ± 0.01 Å for β-C_8Glc and 12.46 ± 0.05 Å for β-C_8Gal was obtained (Table 1). Thus, on the basis of the mean radius of gyration, the two micelles are similar in size. The value of 12.4 Å for β-C_8Glc is in reasonable agreeement with the value of 13.0 Å obtained from a previous simulation of an (β-C_8Glc)$_{27}$ micelle,[18] particularly given the differences in simulation conditions (CHARMM force field and parameters and cubic periodic boundary conditions). Both theoretical values lie within an experimental estimate of R_g of 12 ± 1 Å (we note that this is derived from a gel filtration approach[28]). The calculated values also correspond well to a cylinder radius of 12.7 ± 0.2 Å of prolate micelles of β-C_8Glc obtained from small angle neutron scattering measurements at 298 K.[37]

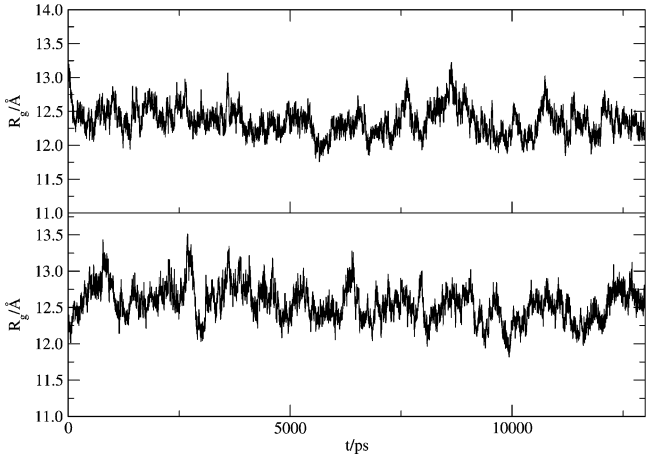

Figure 3. Time series for radius of gyration, R_g, for β-C_8Glc (top) and β-C_8Gal (bottom).

The local density profiles (ldp's) for the simulated β-C_8Glc and β-C_8Gal micelles (Figure 4) are very similar. The headgroup number density maximum at 12.5 Å correlates well with a calculated R_g value of 12.4−12.5 Å. The ldp's also indicate significant penetration of water molecules and, perhaps more surprisingly, alkyl chains into this broad headgroup region, which spans 6−21 Å from the micelle center of mass.

Shape. To provide information on micelle shape, we compute the ratio of the principal moments of inertia, I_1/I_3, where $I_1 > I_2 > I_3$ (Figure 5). As with the radius of gyration, a more converged estimate of the ratio, and the micelle dimensions it represents, is obtained after 5 ns of simulation. Averaging over the last 5 ns of the trajectories, a value of 1.06 for β-C_8Glc and 1.12 for β-C_8Gal is calculated (Table 1). These values are qualitatively consistent with estimates from previous simulation of β-C_8Glc micelles (1.3−1.7)[18] and from other micellar systems (1.0−2.3).[38,39] Averaged axial ratios of the ellipsoidal semiaxes, a/c, are also very similar for β-C_8Glc and β-C_8Gal, as indeed is asphericity, with an ellipticity, e, of 0.5 for both micelles (Table 1). This value of e is consistent with a shape intermediate between a disk/rod ($e = 1$) and an ideal sphere ($e = 0$). That β-C_8Glc micelles are not spherical is in good agreement with available experimental information, including line broadening effects in ^{1}H NMR spectra of micelle growth,[14] as well as from viscosity[40] and heat capacity measurements.[27]

Consistency. Here, we consider the composition of the micelle surface with respect to the proportion of solvent-exposed headgroup and alkyl tail regions. The time evolution of the headgroup, tail, and total solvent-accessible surface areas (Figure 6) appear well equilibrated from the start of the 13 ns production trajectory for both glycolipid−water systems. Nevertheless, to be consistent, we average over the last 5 ns: for β-C_8Gal, we obtain average headgroup and tail solvent-accessible surface areas of 137 ± 2 and 52 ± 0 Å^2 per lipid, respectively (Table 1). Essentially the same values are obtained for the β-C_8Glc micelle (Table 1). Thus, in both cases, nearly 30% of the exposed surface area is due to alkyl chains. The micelles exhibit exposure of large hydrophobic patches (Figure 2).[18,20] Also noted in a previous β-C_8Glc micelle simulation,[18] the theoretical estimate of exposed surface area per lipid obtained (Table 1) considerably exceeds the experimental value (44 Å^2),[13] although the latter is more likely to correspond to lower curvature systems. Additionally, the experimental estimate from small angle scattering measurements[13] considers the hydrophobic−hydrophilic interface (i.e., between glucose and nonpolar tail

TABLE 1: Radius of Gyration, R_g (Å), Ratio of Moments of Inertia, I_1/I_3, Axial Ratio, a/c, Ellipticity, e, and Average Headgroup, A_{head}, and Tail, A_{tail}, Solvent-Accessible Surface Area (Å^2)

micelle	R_g	I_1/I_3	a/c	e	A_{head}	A_{tail}
β-C_8Glc	12.36 ± 0.01	1.06 ± 0.02	1.12 ± 0.08	0.51 ± 0.14	141 ± 2	50 ± 1
β-C_8Gal	12.46 ± 0.05	1.12 ± 0.03	1.14 ± 0.01	0.50 ± 0.03	137 ± 2	52 ± 0

groups) and neglects the known roughness and irregularity of micellar surfaces, as simulated here.

We may conclude that although MD simulations of the water−glycolipid systems appear stable and structural properties converged, there is no major difference in packing of the β-C_8Glc and β-C_8Gal surfactant micelles, as indicated by size, shape, or consistency.

3.2. Microscopic Interactions of Equilibrated Micelles. We now compare the molecular level interactions of β-C_8Glc and β-C_8Gal micelles via analysis of the last 5 ns of the MD trajectories.

Inter-headgroup Hydrogen Bonding. We first consider the hydrogen bonds formed between surfactant headgroups, with the carbohydrate O atoms as acceptor and, where appropriate, the corresponding H atom as donor (Table 2). The total number of inter-headgroup hydrogen bonds per surfactant is 0.89 for β-C_8Glc and 1.07 for β-C_8Gal (Table 2). Although error bars of 0.05 and 0.03 hydrogen bonds respectively imply care in interpretation of these averages, for the final 2.5 ns of the simulations, we find a total number of inter-headgroup hydrogen bonds of 0.90 and 1.07 for β-C_8Glc and β-C_8Gal, which suggests a measure of convergence in these values. A net difference of 0.2 hydrogen bonds would preferentially stabilize the β-C_8Gal micelle by an enthalpy of around 1 kcal/mol per surfactant, based on an estimate of 5 kcal/mol per hydrogen bond. The degree of inter-headgroup hydrogen bonding in $(\beta\text{-}C_8Glc)_{27}$ found here is similar to that observed in a MD simulation of a ternary mixture of decane, water, and *n*-decyl-β-D-glucopyranoside (in lamellae),[21] where an average value of 1.1 inter-headgroup hydrogen bonds per surfactant was found. The similarity again is interesting, considering the different simulation conditions, not the least the influence of the octane component, the brevity of the simulations (400 ps), and the effect of lower curvature.

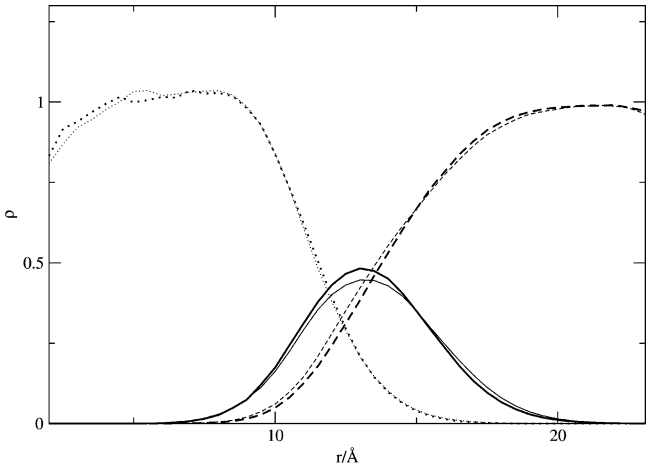

Figure 4. Local density profile of micelle−solvent system: headgroup (solid), lipid tail (dotted), and water (dashed) for β-C_8Glc (bold) and β-C_8Gal.

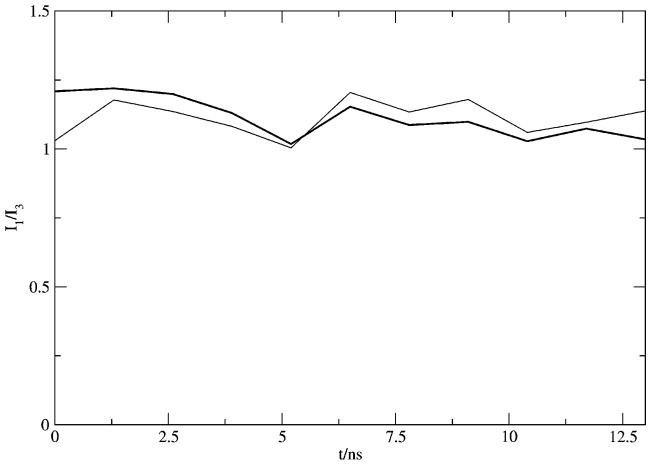

Figure 5. Time series of the ratio of micelle principal moments of inertia, I_1/I_3, for β-C_8Glc (bold) and β-C_8Gal.

Analysis of individual donor and acceptor contributions to hydrogen bonding here indicates generally only small variations between β-C_8Glc and β-C_8Gal headgroups (Table 2). The largest differences are for O3−H of β-C_8Gal, which donates 0.08 more hydrogen bonds and for atom O2 of β-C_8Gal, which accepts 0.06 more hydrogen bonds (Table 2). With an axial orientation of the epimeric O4 oxygen in β-C_8Gal (Figure 1), a slightly increased donor capacity (by 0.07 hydrogen bonds) and acceptor capacity (by 0.03 hydrogen bonds) is observed at O4 from the simulations, relative to β-C_8Glc. For both headgroups, we note that the fraction of accepted hydrogen bonds made by ether-like oxygens O1 and O5 is similar to that of hydroxyl oxygens O3 and O4 but less than that of O2 and O6 (Table 2), suggesting the increased availability of O2 and O6 to accept inter-headgroup hydrogen bonds. Interestingly, a recent molecular dynamics study of concentrated glucose solutions in water (at 1 and 5 *m*) observed a lower proportion of inter-glucose hydrogen bonding at O3, O4, and O5 oxygen acceptors, relative to other oxygens.[41]

Intra-headgroup Hydrogen Bonding. The β-D-galactosyl headgroup of the β-C_8Gal micelle was found to make 1.7 intramolecular hydrogen bonds per surfactant, 0.2 more than in the case of the β-C_8Glc micelle (Table 3). Interestingly, the increased population of intra-lipid hydrogen bonds for β-C_8Gal relative to β-C_8Glc occurs over several interactions, mainly involving the O4 oxygen (0.2 more hydrogen bonds, Table 3). By contrast, the O6−H···O5 interaction in β-C_8Glc accounts

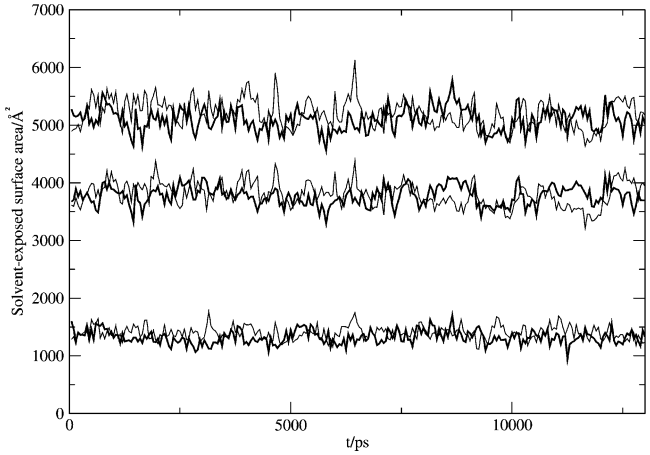

Figure 6. Time series of solvent-exposed surface area: total (top), polar headgroup (middle), and nonpolar tail (bottom) surface area exposed for β-C_8Glc (bold) and β-C_8Gal.

TABLE 2: Fraction of Populated Inter-headgroup and Headgroup−Solvent Hydrogen Bonds per Lipid[a]

	β-C_8Glc				β-C_8Gal				$\Delta(\beta$-C_8Glc − β-C_8Gal)	
	inter-headgp		headgp−solvent		inter-headgp		headgp−solvent			
	donor	acceptor	donor	acceptor	donor	acceptor	donor	acceptor	Δinter-headgp	Δheadgp−solvent
O1		0.15		0.50		0.15		0.52		−0.02
O2	0.34	0.22	0.79	1.10	0.39	0.28	0.74	1.06	−0.05	0.09
O3	0.13	0.10	1.09	1.42	0.21	0.12	0.99	1.41	−0.08	0.11
O4	0.08	0.10	1.14	1.38	0.15	0.13	1.00	1.06	−0.07	0.46
O5		0.10		0.34		0.12		0.46		−0.12
O6	0.34	0.23	0.58	1.42	0.32	0.27	0.61	1.44	0.02	−0.05
total	0.89 ± 0.05	0.90 ± 0.04	3.60 ± 0.03	6.16 ± 0.04	1.07 ± 0.03	1.07 ± 0.03	3.34 ± 0.03	5.95 ± 0.04	−0.18 ± 0.07	0.47 ± 0.06

[a] The standard errors on individual atom contributions range between ±0.00 and ±0.05 hydrogen bonds.

TABLE 3: Fraction of Populated Intra-headgroup Hydrogen Bonds Per Lipid

interaction	β-C_8Glc	β-C_8Gal
O2−H···O1	0.13	0.13
O2−H···O3	0.16	0.19
O3−H···O2	0.23	0.22
O3−H···O4	0.11	0.18
O4−H···O3	0.36	0.40
O4−H···O5	0.00	0.03
O4−H···O6	0.01	0.05
O6−H···O4	0.01	0.06
O6−H···O5	0.50	0.40
total	1.51 ± 0.01	1.66 ± 0.01

for 0.1 more hydrogen bonds than in the case of β-C_8Gal, due to the spatial location of the neighboring 4-OH group.

Headgroup−Water Hydrogen Bonding. The local density profiles indicate considerable interaction between solvent and the carbohydrate headgroups (Figure 4). The β-D-glucosyl headgroup makes on average 9.8 hydrogen bonds to water, and the β-D-galactosyl headgroup, 9.3 (Table 2). In contrast to inter-headgroup interactions, there is a strong preference for water molecules to interact with β-C_8Glc in favor of β-C_8Gal, by 0.5 hydrogen bonds. This is mainly due to increased solvation at O4 of β-C_8Glc of 0.3 accepted and 0.1 donated hydrogen bonds (Table 2), which more than compensates for increased water interaction at O5 of β-C_8Gal (0.1 hydrogen bonds). The greater solvation of the O4 of the glucose moiety found here agrees with a preceding MD study of methyl-β-D-glucoside and methyl-β-D-galactoside in aqueous solution.[42] In that study, the methyl-β-D-glucoside O4 was more solvated by 0.2 hydrogen bonds, although we note that the simulation length was rather short (100 ps).

Water Residence Times. Maximum and average water residence times, t_{max} and t_{av}, respectively, were calculated at each of the six carbohydrate oxygens (Table 4). Using a O···O distance cutoff of 4 Å and a resolution of 0.2 ps (see Methods), an overall t_{av} value of 0.9 and 1.0 ps was found for β-C_8Glc and β-C_8Gal, respectively. This is of the order of average water residence times around the carbohydrates trehalose and sucrose, of up to 0.7 ps as estimated from MD simulations.[43] We noted however that water molecules may instantaneously fluctuate beyond the 4 Å cutoff and yet remain locked within the vicinity of the solute oxygen. Thus, we also considered a lower resolution approach, using configurations at 2 ps intervals in the calculation of residence times. At this coarser-grained level, an extended overall t_{av} value of 4.8 and 4.7 ps was found for β-C_8Glc and β-C_8Gal, respectively (Table 4). Predictably, the longer t_{av} values are found at the hydroxyl oxygens, O2, O3, O4, and O6. Differences in t_{av} between β-C_8Glc and β-C_8Gal micelles however are small.

As with the average residence time, the maximum solvent residence time was calculated at the headgroup oxygens (Table 4). The largest t_{max} value was found for β-C_8Glc, occurring at the O2 oxygen atom. t_{max} values of 164.0 and 127.0 ps were obtained from low and high resolution calculations, respectively, compared to respective t_{max} values of 88.0 and 80.8 ps for β-C_8Gal (Table 4). Long t_{max} values are still obtained using a more stringent 3.5 Å cutoff for calculating solvent interactions: at low and high resolution, the largest t_{max} value is 144.0 and 96.2 ps at O2 for β-C_8Glc and 82.0 and 73.0 ps at O2 for β-C_8Gal, respectively (Supporting Information Table 1S). Waters with a t_{max} value in excess of 25 ps (at low resolution) are rare however (Figure 7). It is interesting that, although rare, there does seem to be a larger number of long-lived waters associated with the β-C_8Glc micelle (Figure 7). These long maximum residence times considerably exceed those found from MD simulation of free monosaccharides in aqueous solution, typically of the order of 10^1 ps. For the disaccharides sucrose and trehalose, maximum residence times of up to 30.6 and 27.2 ps, respectively, were obtained from MD simulations.[43]

The t_{max} values obtained here are more commensurate with values found for water molecules trapped within the crevices and clefts of proteins. For example, for a nanosecond MD simulation of the protein myoglobin,[44] selected water residence times approached 500 ps. However, the majority of solvating water molecules had considerably shorter residence times, in reasonable agreement with water residence times of 10−50 ps obtained from NMR experiments.[45,46] In this work, the longest t_{max} value in the β-C_8Glc simulation corresponds to a water molecule entangled between four carbohydrate moieties in a headgroup cluster (Figure 8). Similarly, in the β-C_8Gal micelle

TABLE 4: Maximum, t_{max}, and Average, t_{av}, Water Residence Times (ps)

	β-C_8Glc				β-C_8Gal			
	t_{max}[a]	t_{max}[b]	t_{av}[a]	t_{av}[b]	t_{max}[a]	t_{max}[b]	t_{av}[a]	t_{av}[b]
O1	41.0	116.0	0.65 ± 0.02	4.33 ± 0.16	28.4	44.0	0.63 ± 0.02	3.97 ± 0.11
O2	127.0	164.0	1.21 ± 0.06	5.86 ± 0.20	80.8	88.0	1.70 ± 0.05	5.52 ± 0.18
O3	52.4	82.0	1.13 ± 0.03	5.20 ± 0.11	41.6	76.0	1.09 ± 0.03	4.92 ± 0.10
O4	57.2	64.0	1.01 ± 0.02	4.58 ± 0.09	71.8	88.0	0.99 ± 0.02	4.67 ± 0.11
O5	41.6	66.0	0.69 ± 0.03	4.18 ± 0.15	50.4	82.0	0.85 ± 0.03	4.64 ± 0.19
O6	67.0	68.0	0.94 ± 0.03	4.57 ± 0.11	45.6	66.0	0.95 ± 0.03	4.55 ± 0.10

[a] Resolution of 0.2 ps. [b] Resolution of 2.0 ps.

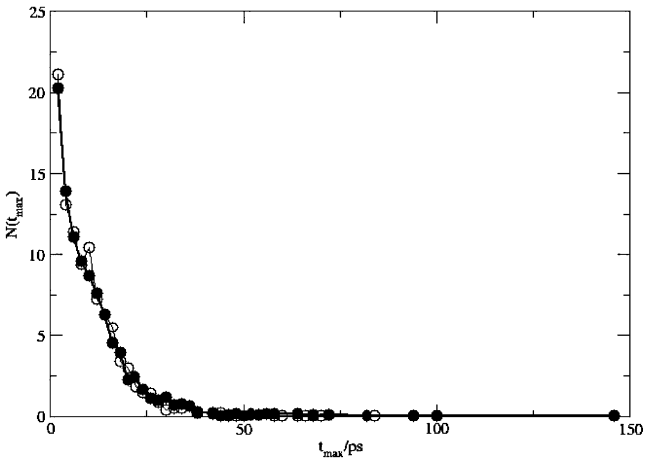

Figure 7. Distribution profile, *N*, of maximum residence time for β-C_8Glc (bold) and β-C_8Gal using a 3.5 Å O···O cutoff. For $t_{max} > 40$ ps, circles indicate nonzero residence times, for β-C_8Glc (filled) and β-C_8Gal (clear).

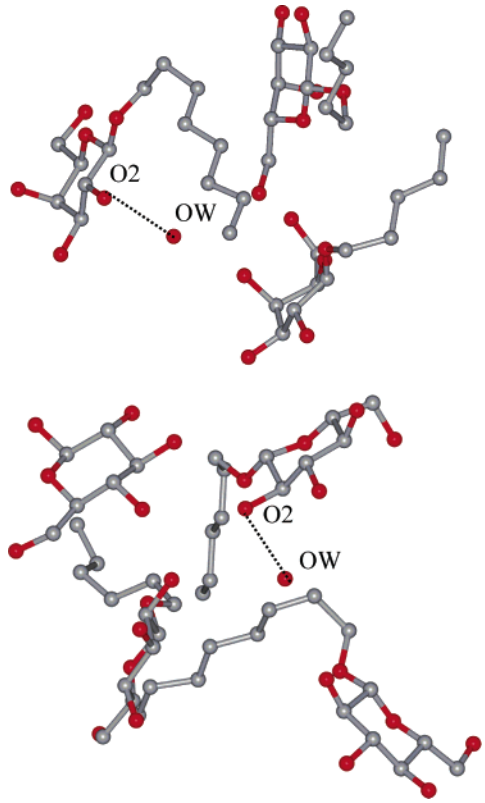

Figure 8. MD snapshot of long-lived interaction of water with (top) three headgroups of β-C_8Gal ($t_{max} = 88$ ps at a 4.0 Å cutoff and 82 ps at a 3.5 Å cutoff); (bottom) four headgroups of β-C_8Glc ($t_{max} = 164$ ps at a 4.0 Å cutoff and 144 ps at a 3.5 Å cutoff).

simulation, the water with the largest maximum residence time (88 ps, Table 4) is engaged by three carbohydrate headgroups (Figure 8). For both long-lived waters, we note that they interact with the micelle at a site of glycolipid protrusion. The roughness of the micelle surface (Figure 2) appears to promote solvent entanglement and is perhaps analogous to the hydration sites found in protein clefts.

4. Discussion

For MD simulation of $(\beta$-C_8Glc$)_{27}$ and $(\beta$-C_8Gal$)_{27}$ micelles, we observe that convergence in some properties requires long equilibration times (>5 ns). A recent MD simulation of a ganglioside bilayer[19] found an equilibration time of around 30 ns was necessary. This longer equilibration time was in part a function of the more complex trisaccharide headgroup, arising from slow relaxation of a glycosidic linkage between sugar residues. Once converged, the micelle MD simulations here indicate similar overall shape, size, and exposed headgroup/tail distributions for β-C_8Glc and β-C_8Gal. The simulations generally correspond well to measurements obtained from small angle scattering, NMR, and other experimental studies. We also note that the simulations predict up to ~30% of micelle surface area exposed to solvent belongs to alkyl chains. It has been estimated that the free energy cost for exposed hydrophobic surface area is 104 cal/(mol $Å^{-2}$).[47] Thus, using the estimates of exposed alkyl tail surface area for β-C_8Glc and β-C_8Gal (Table 1), this energetic penalty amounts to 144.9 kcal/mol (β-C_8Gal) and 140.6 kcal/mol (β-C_8Glc). The net solvation free energy is favorable, however, amply compensated by favorable headgroup hydrogen bonding interactions with solvent, with an average of 10 hydrogen bonds formed by each of the 27 headgroups (Table 2). Nevertheless, we note that the carbohydrate headgroups themselves are not uniformly hydrophilic. For example, carbohydrates frequently form stacked hydrophobic interactions with proteins.[48] Thus, the calculation of solvent-exposed surface area of the alkyl chains here should be considered a lower limit for exposed hydrophobic surface area.

Similarly, there is little difference in the net number of hydrogen bonds calculated between headgroups for the two micelle systems (Table 2), although simulation suggests that β-C_8Gal is a slightly better donor (mainly at O3) and acceptor (mainly at O2) than β-C_8Glc. The clear distinction in the microscopic behavior of β-C_8Glc and β-C_8Gal micelles, however, lies in the interaction of headgroups with solvent, with the main difference occurring at the O4 oxygen, and to a lesser extent O5. This arises principally from an increased acceptor capacity of β-C_8Glc. Relative to β-C_8Glc, the smaller solvent interaction at O4 of the galactosyl headgroup by about 0.4 hydrogen bonds (Table 2) correlates with increased inter- and intra-headgroup hydrogen bonding at O4 by the same number of bonds (Tables 2 and 3).

The greater water interaction due to the stereochemistry of the glucose moiety, also suggested here by longer calculated water residence times at the β-C_8Glc micelle, may be related to a theory[49] in which the 3D spatial location of oxygens in glucose is deemed a better complement to the averaged structure of water (in a sense, a "solvaphoric" arrangement of atoms). Thus, a β-glucose O2···O4 distance of 4.9 Å in the crystal is more commensurate with the second peak in the water radial distribution function (4.8 Å), compared to the crystallographic value in β-galactose of 4.3 Å.[50] This also correlates with a slightly different partial molar volume for D-glucose and D-galactose at infinite dilution (111.7 and 110.2 cm^3 mol^{-1}, respectively); compressibility studies also suggest galactose is less well accommodated within the structure of water.[51,52] Our simulation results and this theory are further supported by the increased water solubility of glucose over galactose, with solubilities at 293 K of 45.1 and 40.6 wt %, respectively.[51] The observed preference of stronger glucose−water interactions and a higher proportion of intra- and inter-galactose hydrogen bonding could explain, at larger surfactant concentrations, the greater ease with which the lyotropic phase transition from crystal to L_α occurs for β-C_8Glc relative to β-C_8Gal.

5. Conclusions

MD simulations of $(\beta$-C_8Glc$)_{27}$ and $(\beta$-C_8Gal$)_{27}$ micelles exhibit stability and similar properties. The most significant

difference in simulated micelle behavior lies in the O4−water interaction, which is considerably greater for β-C_8Glc surfactants. This correlates with experimental measurements including solubilities and partial molar compressibilities[52] which indicate that the stereochemistry of galactose leads to a stronger perturbation of water structure than in the case of glucose. For both surfactants, simulations also identify long-lived water interactions at surface protrusions involving headgroup clusters (Figure 8).

The predicted net hydrogen bonding between sugar unit headgroups in β-C_8Gal and β-C_8Glc micelles is similar, although β-C_8Gal has slightly more extensive inter-surfactant and intramolecular hydrogen bonding. Therefore, fractionally greater hydrogen bonding between galactosyl headgroups may preferentially stabilize the β-C_8Gal micelles enthalpically (by an estimated 1 kcal/mol per unit) and contribute, at least in part,[53] to higher T_m and T_c values than those observed for β-C_8Glc in lyotropic systems. However, care is required in the extension of these simulation results to interpretation of T_m and T_c at higher lipid concentrations. At higher lipid concentrations, where extended lamellar structures are formed, curvature will reduce and this may influence the ratio of inter-solute and solvent hydrogen bonding. Therefore, to explore the extent of these effects and provide further insight into the differing T_m and T_c values of alkyl glycoside systems, work is underway to investigate the influence of varying carbohydrate headgroup, lipid concentration, and temperature via MD simulation of glycolipid bilayers. As structure−property relationships are established for glycolipid systems, the aim is to enable design of glycolipid systems where physical properties can be tuned via headgroup structure, permitting development of synthetic glycolipids suitable for a range of applications in nanotechnology, including engineered protein recognition by glycolipids.

Acknowledgment. We gratefully acknowledge grants from the Malaysian Ministry of Science, Technology and Innovation (09-02-0309010 SR0004/04) and from the EPSRC for HPCx supercomputing time. We also thank Prof. J. M. Seddon, Prof. G. J. T. Tiddy, and Dr. C. W. Yong for helpful discussions.

Supporting Information Available: Table showing maximum and average residence times for β-C_8Glc and β-C_8Gal. This material is available free of charge via the Internet at http://pubs.acs.org.

References and Notes

(1) Raulin, J. *Prog. Lipid Res.* **2002**, *41*, 27−65.
(2) Yuki, I.; Irimura, T. *Mol. Med.* **1994**, *31*, 1278−1284.
(3) Lencer, W. I.; Tsai, B. *Trends Biochem. Sci.* **2003**, *28*, 639−645.
(4) Hantgan, R. R.; Braaten, J. V.; Rocco, M. *Biochemistry* **1993**, *32*, 3935.
(5) Conlan, S.; Bayley, H. *Biochemistry* **2003**, *42*, 9453−9465.
(6) Kitamoto, D.; Isoda, H.; Nakahara, T. *J. Biosci. Bioeng.* **2002**, *94*, 187−201.
(7) Jones, M. N. *Adv. Drug Delivery Rev.* **1994**, *13*, 215−249.
(8) Inouye, M.; Waki, M.; Abe, H. *J. Am. Chem. Soc.* **2004**, *126*, 2022−2027.
(9) Matsumara, S.; Imai, K.; Yoshikawa, S.; Kawada, K.; Uchibori, T. *J. Am. Oil Soc.* **1990**, *67*, 996−1001.
(10) Hato, M.; Minamikawa, H.; Tamda, K.; Baba, T.; Tanabe, Y. *Adv. Colloid Interface Sci.* **1999**, *80*, 233−270.
(11) Sakya, P.; Seddon, J. M.; Vill, V. *Liq. Cryst.* **1997**, *23*, 409−424.
(12) Sakya, P.; Seddon, J. M.; Templer, R. H. *J. Phys. II* **1994**, *4*, 1311−1331.
(13) Nilsson, F.; Soderman, O.; Johansson, I. *Langmuir* **1996**, *12*, 902−908.
(14) Bonicelli, M.; Ceccaroni, G. F.; La Mesa, C. *Colloid Polym. Sci.* **1998**, *276*, 109−116.
(15) Naidoo, K. J.; Brady, J. W. *J. Am. Chem. Soc.* **1999**, *121*, 2244−2252.
(16) Brady, J. W.; Schmidt, R. K. *J. Phys. Chem.* **1993**, *97*, 958−966.
(17) Corzana, F.; Motawia, M. S.; Herve de Penhoat, C.; Perez, S.; Tschampel, S. M.; Woods, R. J.; Engelsen, S. B. *J. Comput. Chem.* **2004**, *25*, 573−586.
(18) Bogusz, S.; Venable, R. M.; Pastor, R. W. *J. Phys. Chem. B* **2000**, *104*, 5462−5470.
(19) Sega, M.; Vallauri, R.; Brocca, P.; Melchionna, S. *J. Phys. Chem. B* **2004**, *108*, 20322−20330.
(20) Bogusz, S.; Venable, R. M.; Pastor, R. W. *J. Phys. Chem. B* **2001**, *105*, 8312−8321.
(21) van Buuren, A. R.; Berendsen, H. J. C. *Langmuir* **1994**, *10*, 1703−1713.
(22) Focher, B.; Savelli, G.; Torri, G.; Vecchio, G.; McKenzie, D. C.; Nicoli, D. F.; Burton, C. A. *Chem. Phys. Lett.* **1989**, *158*, 491−494.
(23) Woods, R. J.; Dwek, R. A.; Edge, C. J.; Fraser-Reid, B. *J. Phys. Chem.* **1995**, *99*, 3832−3846.
(24) Pathiaseril, A.; Woods, R. J. *J. Am. Chem. Soc.* **2000**, *122*, 331−338.
(25) Cornell, W. D.; Cieplak, P.; Bayly, C. I.; Gould, I. R.; Merz, K. M., Jr.; Ferguson, D. M.; Spellmeyer, D. C.; Fox, T.; Caldwell, J. W.; Kollman, P. A. *J. Am. Chem. Soc.* **1995**, *117*, 5179−5197.
(26) Jorgensen, W. L.; Chandrasekhar, J.; Madura, J. D.; Impey, R. W.; Klein, M. L. *J. Chem. Phys.* **1983**, *79*, 926−935.
(27) D'Aprano, A.; Giordano, R.; Jannelli, M. P.; Magazu, S.; Maisano, G.; Sesta, B. *J. Mol. Struct.* **1996**, *383*, 177.
(28) vanAken, T.; Foxall-vanAken, S.; Castleman, S.; Ferguson-Miller, S. *Methods Enzymol.* **1986**, *125*, 27.
(29) Hussan, S.; Rowe, W.; Tiddy, G. J. T. Surfactant Liquid Crystals and Surfactant Chemical Structure. In *Handbook of Applied Surface and Colloid Chemistry*; Holmberg, K., Ed.; John Wiley & Sons: New York, 2001; Chapter 21, pp 465−508.
(30) Lorber, B.; Bishop, J. B.; DeLucas, L. *Biochim. Biophys. Acta* **1990**, *1023*, 254.
(31) Case, D. A.; Darden, T.; Cheatham, T. E., III; Simmerling, C. L.; Wang, J.; Duke, R.; Luo, R.; Merz, K. M., Jr.; Wang, B.; Pearlman, D. A.; Crowley, M.; Brozell, S.; Tsui, V.; Gohlke, H.; Mongan, J.; Hornak, V.; Cui, G.; Beroza, P.; Schafmeister, C.; Caldwell, J. W.; Ross, W. S.; Kollman, P. A. *AMBER 8.0*; University of California, San Francisco: San Francisco, CA, 2004.
(32) Berendsen, H. J. C.; Postma, J. P. M.; van Gunsteren, W. F.; DiNola, A.; Haak, J. R. *J. Chem. Phys.* **1984**, *81*, 3684−3690.
(33) Ryckaert, J. P.; Ciccotti, G.; Berendsen, H. J. C. *J. Comput. Phys.* **1977**, *23*, 327−341.
(34) Hubbard, S. J.; Thornton, J. M. *NACCESS*; Department of Biochemistry and Molecular Biology, University College London, 1993.
(35) Lee, B.; Richards, F. M. *J. Mol. Biol.* **1971**, *55*, 379−400.
(36) Israelachvilli, J.; Wennerstrom, H. *Langmuir* **1990**, *6*, 873−876.
(37) He, L. Z.; Garamus, V. M.; Niemeyer, B.; Helmholz, H.; Willumeit, R. *J. Mol. Liq.* **2000**, *89*, 239−249.
(38) Shelley, J.; Watanabe, K.; Klein, M. L. *Int. J. Quantum Chem.* **1990**, *S17*, 103−117.
(39) Shelley, J. C.; Sprik, M.; Klein, M. L. *Langmuir* **1993**, *9*, 916.
(40) Bonincontro, A.; Briganti, G.; D'Aprano, A.; La Mesa, C.; Sesta, B. *Langmuir* **1996**, *12*, 3206.
(41) Mason, P. E.; Neilson, G. W.; Enderby, J. E.; Saboungi, M.-L.; Brady, J. W. *J. Phys. Chem. B* **2005**, *109*, 13104−13111.
(42) Cheetham, N. W. H.; Lam, K. *Carbohydr. Res.* **1996**, *282*, 13−23.
(43) Engelsen, S. B.; Monteiro, C.; Herve de Penhoat, C.; Perez, S. *Biophys. Chem.* **2001**, *93*, 103−127.
(44) Makarov, V. A.; Andrews, B. K.; Smith, P. E.; Pettitt, B. M. *Biophys. J.* **2000**, *79*, 2966−2974.
(45) Brunne, R. M.; Liepinsh, E.; Otting, G.; Wuthrich, K.; an Gunsteren, W. F. *J. Mol. Biol.* **1993**, *231*, 1040−1048.
(46) Denisov, V. P.; Halle, B. *Faraday Discuss.* **1996**, *103*, 227−244.
(47) Cramer, C. J.; Truhlar, D. G. *Science* **1992**, *256*, 213−217.
(48) Weis, W. I.; Drickamer, K. *Annu. Rev. Biochem.* **1996**, *65*, 441−473.
(49) Galema, S. A.; Blandamer, M. J.; Engberts, J. B. F. N. *J. Am. Chem. Soc.* **1990**, *112*, 9665−9666.
(50) Galema, S. A.; Howard, E.; Engberts, J. B. F. N.; Grigera, J. R. *Carbohydr. Res.* **1994**, *265*, 215−225.
(51) Ces, O.; Seddon, J. M.; Templer, R. H.; Mannock, D. A.; McElhaney, R. N. Differential Scanning Calorimetry and X-ray Diffraction Studies of Glycolipid Membranes. In *Probing and modelling membranes and proteins*; Templer, R., Leatherbarrow, R. J., Eds.; RSC publications: Cambridge, U.K., 2001.
(52) Galema, S. A.; Hoiland, H. *J. Phys. Chem.* **1991**, *95*, 5321−5326.
(53) Vill, V.; Bocker, T.; Thiem, J.; Fischer, F. *Liq. Cryst.* **1989**, *6*, 349.